Extraction of Thermodynamic Parameters of Protein Unfolding using Parallelized Differential Scanning Fluorimetry

Thaiesha A. Wright, Jamie M. Stewart, Richard C. Page, and Dominik Konkolewicz**

Department of Chemistry and Biochemistry, Miami University, Oxford, OH 45056, United States

AUTHOR INFORMATION

Corresponding Author

*Richard C. Page (pagerc@miamioh.edu). *Dominik Konkolewicz (konkold@miamioh.edu).

ABSTRACT

Thermodynamic properties of protein unfolding have been extensively studied; however, the methods used have typically required significant preparation time and high protein concentrations. Here, we present a facile, simple, and parallelized differential scanning fluorimetry (DSF) method that enables thermodynamic parameters of protein unfolding to be extracted. This method assumes a two-state, reversible protein unfolding mechanism and provides the capacity to quickly analyze the biophysical mechanisms of changes in protein stability and to more thoroughly characterize the effect of mutations, additives, inhibitors, or pH. We show the utility of the DSF method by analyzing the thermal denaturation of lysozyme, carbonic anhydrase, chymotrypsin, horseradish peroxidase, and cellulase enzymes. Compared to similar biophysical analyses by circular dichroism, DSF allows for determination of thermodynamic parameters of unfolding while providing greater than 24-fold reduction in experimental time. This study opens to door to rapid characterization of protein stability on low concentration protein samples.

TOC GRAPHICS

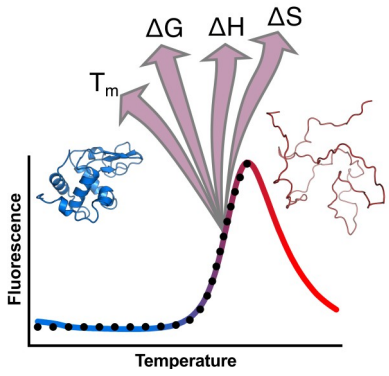

KEYWORDS

Protein stability, denaturation, free energy, enthalpy, entropy, melting temperature.

Although the melting temperature (T_m) of a protein is often used as a proxy for stability, the Gibbs free energy of unfolding ($\Delta_u G$) is a more thermodynamically correct measure of protein stability[1]. When paired with T_m, determining $\Delta_u G$ allows for extraction of the enthalpy of unfolding ($\Delta_u H$) and entropy of unfolding ($\Delta_u S$). Numerous techniques have been utilized for estimating $\Delta_u G$, including chemical denaturation[2-8], differential scanning calorimetry (DSC)[5-10], differential scanning fluorimetry (DSF)[10], hydrogen-deuterium exchange mass spectrometry (HDX-MS)[11], and thermal denaturation[12]. However, the bulk of these techniques entail significant preparation time, require high concentrations of protein, and necessitate nontrivial optimization. In this study, we address this issue by presenting a parallelized DSF approach that enables a set of thermodynamic parameters of protein unfolding to be extracted for proteins assuming a reversible, two-state unfolding model. The advantages of this technique include: general applicability to many proteins, the small quantity of protein required, and the ability to parallelize measurements. These advantages allow for high multiplicity of experimental conditions, providing the ability to assess protein stability with respect to various additives, inhibitors, or pH values simultaneously.

The T_m value for any given protein represents the temperature at which the protein is 50% folded[13-14]. At this temperature, the Gibbs free energy of the folded and unfolded states are equivalent, and $\Delta_u G$ is zero. Melting temperatures can be readily determined using various biophysical techniques such as DSC[15-19], DSF[20-24], circular dichroism (CD)[24-27], or Fluorescence[28-32]. However, conclusive determination protein stability cannot be obtained from simple determination of the midpoint of the folded-to-unfolded transition (T_m)[33]. For example, cytochrome c exhibits a T_m of 80 °C, which would intuitively suggest it more stable than lysozyme which exhibits a T_m of 74 °C[34]; however, under standard conditions the $\Delta_u G$ lysozyme (50.2 kJ mol^{-1}) is 16.7 kJ mol^{-1} higher than the $\Delta_u G$ for cytochrome c (33.5 kJ mol^{-1})[33]. Thus, assessing protein stability requires more than a simple comparison of T_m. Below we discuss an approach that extracts $\Delta_u G$, $\Delta_u H$, and $\Delta_u S$ from the slope of the folded-to-unfolded transition as measured by DSF.

Unfolding of the proteins reported herein are approximated with a two-state transition from the native, fully folded state to the unfolded state where the hydrophobic core is solvent exposed. Although several proteins involve multiple intermediate states[35-38], it will be shown through benchmarking experiments that the two-state approximation is sufficient to recapitulate $\Delta_u G$ values reported in the literature, even for complex proteins. It is worth noting that for proteins that follow a two state folded/unfolded denaturation, the outlined method will provide true thermodynamic parameters. In contrast, for proteins that follow more complex denaturation pathways involving intermediates, the outlined method will provide apparent thermodynamic parameters that approximate those that explicitly consider intermediates. Nevertheless, we will show that this DSF based method is capable of extracting $\Delta_u G$ with acceptable agreement to literature values across a wide range of simpler and complex proteins. Finally, we highlight the potential of our method, by estimating thermodynamic parameters for a library of cellulase mutants in parallel.

DSF reports fluorescence intensity as a function of temperature for protein samples incubated with a solvatofluorochromic dye[39]. We use the merocyanine dye SYPRO Orange that exhibits a substantial increase in fluorescence quantum yield upon partitioning from aqueous solution into a hydrophobic environment with a reduced dielectric constant[40]. Since the fluorescence can be measured at each temperature, this fluorescence can be converted to an equilibrium constant of unfolding. With knowledge of the equilibrium constant, which can be converted to the Gibbs free energy of unfolding ($\Delta_u G$) near the protein's melting point, it is possible to extrapolate and estimate the Gibbs free energy of unfolding at any other temperature.

DSF data up to the maximal fluorescence value is fitted using a Boltzmann function (eq. 1) in Prism (GraphPad, Inc.) with least squares minimization, where F_{min} is the minimal fluorescence value, T is the temperature, T_m is the protein's melting temperature, and m is a parameter to characterize the breadth of the transition.

$$F_{calc} = F_{min} + \frac{F_{max} - F_{min}}{1 + e^{\left(\frac{T_m - T}{m}\right)}} \qquad (1)$$

Alternative estimates of T_m from the DSF data can be obtained as the point of inflection on the increasing portion of the DSF curve, or the mid-point between minimal and maximal fluorescence on the DSF curve. Provided with T_m, the fraction of the protein that remains folded, P_f, is calculated at each temperature as:

$$P_f = 1 - \frac{F - F_{min}}{F_{max} - F_{min}} \quad (2)$$

Equation 2 assumes a two state model for the protein denaturation. The value for F_{max} is the calculated fluorescence intensity of the fully denatured protein, where P_f is zero while the measured value for F_{min} coincides with P_f equal to 1. Aggregation of unfolded proteins excludes SYPRO Orange from interacting with hydrophobic residues resulting in fluorescence quenching by aqueous solution, which decreases the observed fluorescence, and lowers the value that would be obtained if all unfolded proteins were to interact with the dye. To correct for this behavior we use F_{T_m}, fluorescence intensity at the melting temperature (T_m) and the definition that at T_m 50% the protein is folded to find F_{max} as

$$F_{max} = \left(F_{T_m} - F_{min}\right) + F_{T_m} \quad (3)$$

Given P_f at each temperature, P_u, the fraction of unfolded protein, is calculated as

$$P_u = 1 - P_f \quad (4)$$

The equilibrium constant of unfolding, K_u, may then be calculated utilizing the relationship

$$K_u = \frac{P_u}{P_f} \quad (5)$$

The Gibbs free energy of unfolding, $\Delta_u G$, is calculated using eq. 6 where R is the universal gas constant (8.314 J K^{-1} mol^{-1}), T is the absolute temperature value at each fluorescence intensity, and K_u is the equilibrium constant of unfolding at temperature T as calculated with eq. 5.

$$\Delta_u G = -RT \ln K_u \quad (6)$$

Calculated $\Delta_u G$ values are plotted against temperature values corresponding to 10-50% unfolding. Solving for the linear equation of best fit enables $\Delta_u G$, $\Delta_u S$, and $\Delta_u H$ to be calculated.

Values of R^2 significantly below 0.9 indicate that this methodology is not valid for the protein studied. Potential reasons include a distinct intermediate folded structure, leading to two measurable unfolding steps. It is important to note that in many cases proteins with intermediates can be treated and often appear as simpler two state folded/unfolded systems, since the intermediate is often a minor component due to its metastable nature. In these cases, this DSF methodology would be applicable and yield meaningful thermodynamic parameters.

We report the standard Gibbs free energy of protein unfolding, $\Delta_u G°$, as the value of $\Delta_u G$ extrapolated back to 298K using the line of best fit from the plot of $\Delta_u G$ versus temperature. Best-fit lines use eq. 7, where a is the slope of the line, T is temperature, and b is the y-intercept.

$$\Delta_u G = aT + b \qquad (7)$$

Once $\Delta_u G°$ is determined, $\Delta_u S^o$, the entropy of protein unfolding is determined as:

$$\Delta_u S = \frac{\Delta_u G}{(T_m - T)} \qquad (8)$$

The enthalpy of protein unfolding, $\Delta_u H^o$, is then calculated using the relationship:

$$\Delta_u H = T_m \Delta_u S \qquad (9)$$

It is important to note that in the above analysis the change in heat capacity upon folding is not explicitly determined[41], although it may be included implicitly in the enthalpic and entropic terms. The heat capacity is not explicitly accounted for to minimize the number of fitted parameters, and to provide the simplest model that provides thermodynamic parameters of unfolding that can be used to compare a library of proteins. As indicated in the subsequent section, even with the assumptions in place, the results of our study are broadly consistent with literature data on a variety of proteins.

A series of benchmarking experiments were performed to identify the potential of this method, and compare the results to those reported in the literature for a family of commonly used proteins: carbonic anhydrase, chymotrypsin, lysozyme, and peroxidase. DSF thermal stability curves for carbonic anhydrase, chymotrypsin, lysozyme, and peroxidase are shown in Figure 1. The Boltzmann non-linear regression allows for fitting without requiring baseline subtraction and

provides the T_m. DSF curves were measured in triplicate, yielding small differences in T_m, typically 0.3 °C or smaller, as reported in Table 1.

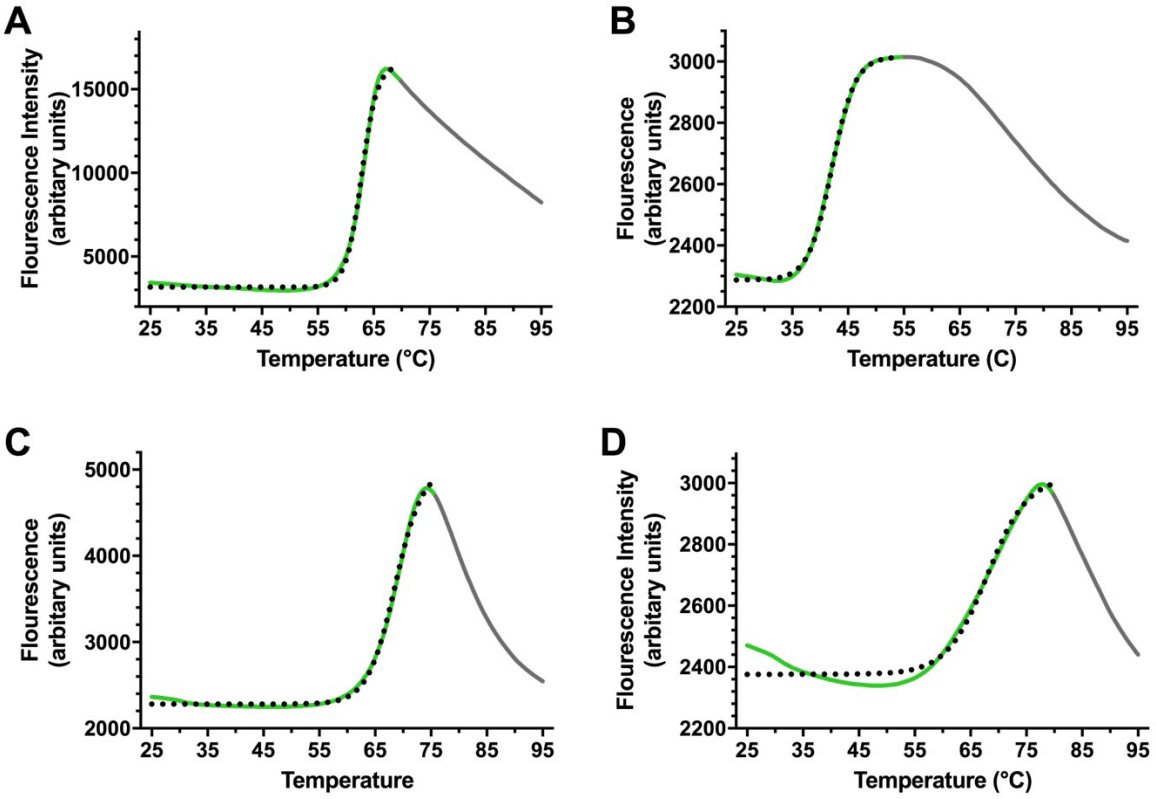

Figure 1. Differential Scanning Fluorimetry of carbonic anhydrase isozyme II from bovine erythrocytes (A), α-chymotrypsin from bovine pancreas (B), hen egg white lysozyme (C), and horseradish peroxidase type I (D) were used to determine T_m, $\Delta_u G°$, $\Delta_u S°$, and $\Delta_u H°$. A Boltzmann fit (dotted line) enabled determination of T_m and spreadsheet calculations were used to estimate $\Delta_u G°$, $\Delta_u S°$, and $\Delta_u H°$ reported in Table 1. Regions of the DSF curve used for Boltzmann fitting are shown green, the gray portion of each DSF curve indicates the region in which aggregation diminishes the observed fluorescence and therefore was not used in fitting.

T_m values from Boltzmann fits were used in eq. 3 for finding F_{max}, allowing for the fraction folded, P_f, fraction unfolded, P_u, and the equilibrium constant for unfolding to be determined using eq 2, 4, and 5, respectively. $\Delta_u G$ values calculated via eq. 6 were plotted against temperature values in the range of 10%-50% unfolded protein (Figure 2). These values were

chosen to minimize issues arising from signal to noise variations at low proportions of unfolded protein, and to minimize the impact of protein aggregation and exclusion of the fluorescent dye at high fractions of unfolded protein. Individual raw fits are given in Supporting Information as Figure S1. Linear fitting with eq. 7 typically exhibits R^2 values of 0.99 or higher and enables $\Delta_u G°$, $\Delta_u S°$, and $\Delta_u H°$ to be calculated using eqs. 6, 7, and 8, respectively (Table 1).

Table 1. Thermal Stability and Thermodynamic data for Carbonic Anhydrase, Chymotrypsin, Lysozyme, and Peroxidase.

Protein	T_m (°C)	$\Delta_u G°$ (kJ/mol)[a]	$\Delta_u S°$ (kJ/mol K) [a]	$\Delta_u H°$ (kJ/mol) [a]
carbonic anhydrase[b]	62.8 ± 0.1	60.4 ± 0.6	1.60 ± 0.02	536 ± 6
chymotrypsin[c]	42.1 ± 0.1	20.7 ± 0.3	1.21 ± 0.02	382 ± 6
lysozyme[d]	68.6 ± 0.1	42.7 ± 0.3	0.98 ± 0.01	335 ± 2
peroxidase[e]	64.1 ± 0.3	24.6 ± 0.5	0.63 ± 0.01	212 ± 5

[a]Δ_uG, Δ_uS, and Δ_uH are the Gibbs free energy of unfolding, entropy of unfolding, and enthalpy of unfolding, respectively. Reported values represent the average of three replicates, and the uncertainty is reported as one standard deviation.

[b]Carbonic anhydrase isozyme II from bovine erythrocytes (pH 7.4).

[c]α-Chymotrypsin from bovine pancreas (pH 3).

[d]Hen egg white lysozyme (pH 7).

[e]Horseradish peroxidase type I (pH 5.5).

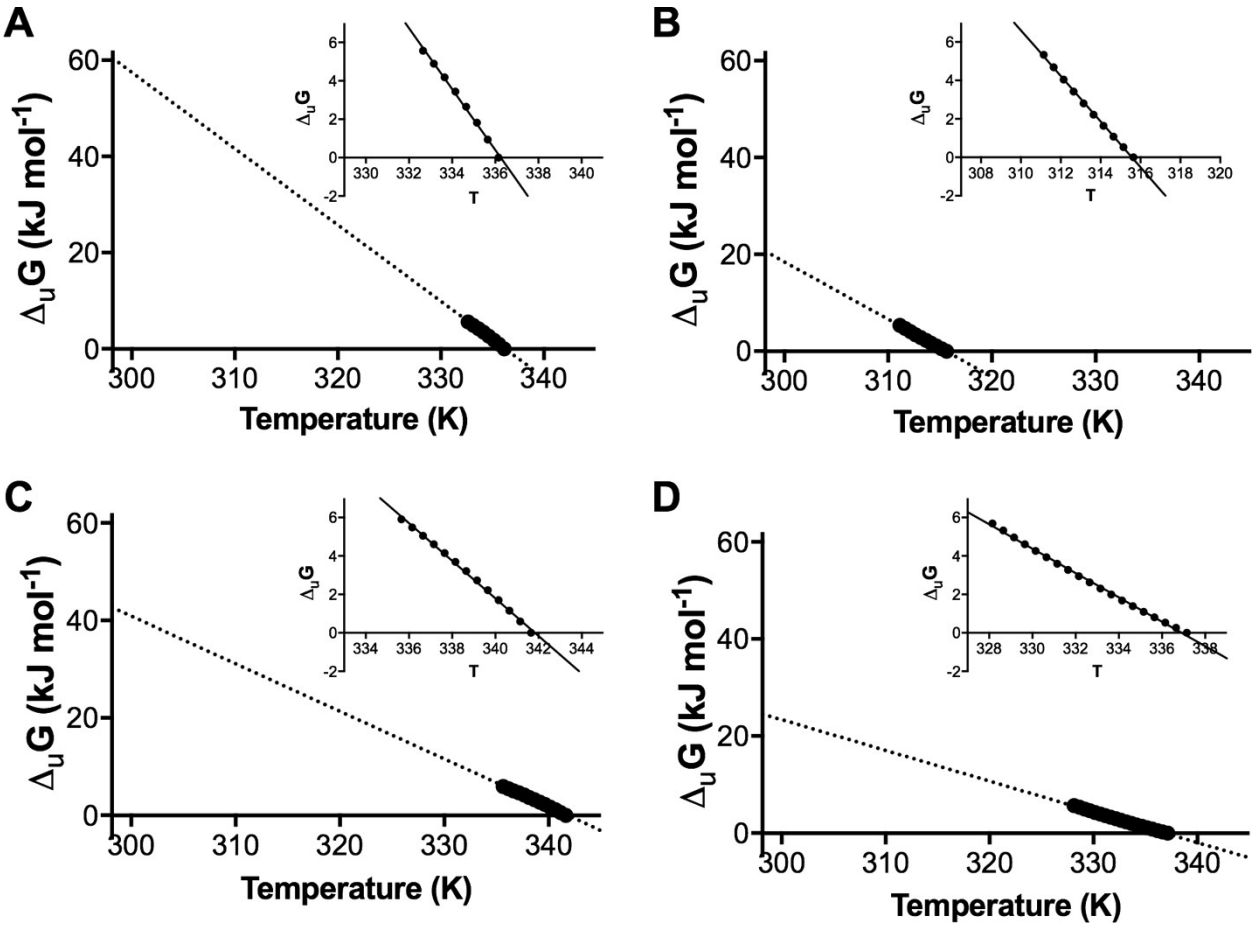

Figure 2. Fitting of DSF data to equation 6 for (A) carbonic anhydrase isozyme I from bovine erythrocytes at pH 7.4, (B) α-chymotrypsin from bovine pancreas at pH 3, (C) hen egg white lysozyme at pH 7, and (D) horseradish peroxidase type I at pH 5.5. R^2 values calculated using excel (Figure S1).

DSF thermal stability curves allow for the calculation of $\Delta_u G°$, $\Delta_u S°$, and $\Delta_u H°$ values with relatively small standard deviations. Despite the high precision, benchmarking the accuracy of the method is difficult due to the overwhelming variability of $\Delta_u G°$ values reported in the literature. However, the $\Delta_u G°$ values reported in Table 1 did fall within the range of reported values in the literature. The calculated value of $\Delta_u G°$ for carbonic anhydrase (b-CA1) of $\Delta_u G°$ = 60.4 ± 0.3 kJ mol^{-1} from the DSF method can be compared to literature values including $\Delta_u G$ = 9.2 kJ mol^{-1} at 60 °C and $\Delta_u G°$ = 59 kJ mol^{-1} at 25 °C using a linear extrapolation method, $\Delta_u G°$ = 71 kJ mol^{-1} by urea denaturation[42] and $\Delta_u G°$ = 75 kJ mol^{-1} using guanidine hydrochloride

denaturation[42]. The $\Delta_u G°$ for chymotrypsin of $\Delta_u G° = 20.7 \pm 0.3$ kJ mol^{-1} from the DSF method can be compared to literature reported $\Delta_u G°$ values for chymotrypsin which include 35.0 kJ mol^{-1} by DSC and 18.15 kJ mol^{-1} via fluorescence spectroscopy[43], 33 kJ mol^{-1} by guanidine hydrochloride denaturation and 35 kJ mol^{-1} by urea denaturation. The $\Delta_u G°$ for lysozyme of $\Delta_u G° = 42.7 \pm 0.3$ kJ mol^{-1} from the DSF method lies within the literature range of $\Delta_u G°$ values for lysozyme which include 37.18 kJ mol^{-1} using guanidine hydrochloride denaturation, 22.9 kJ mol^{-1} for opening lysozyme using HDX-MS, and 46 kJ mol^{-1} by CD[12]. Finally, $\Delta_u G°$ for peroxidase of $\Delta_u G° = 24.6 \pm 0.5$ kJ mol^{-1} from the DSF method can be compared to literature reported $\Delta_u G°$ values for peroxidase which include 24.8 kJ mol^{-1} by urea denaturation[2], 26.2 kJ mol^{-1} using guanidine hydrochloride denaturation[2], 25.6 kJ mol^{-1} using SDS denaturation[8], and 26.9 kJ mol^{-1} using DTAB denaturation[8]. A summary of these $\Delta_u G°$ values determined by this DSF and other methods in the literature is given as Table S1. Thus, with exception of horseradish peroxidase, reported $\Delta_u G°$ values indicate high variability between the various denaturation methods. It is important to note that the estimated values by this technique fall comfortably within the reported ranges in the literature. This agreement with literature ranges is noteworthy, since the outlined approach assumes a two-state model, where the protein transitions directly between the folded and unfolded states without any stable intermediates. Despite the assumption of a two-state model, the thermodynamic parameters obtained are in broad agreement with those reported in the literature for all proteins studied.

Another important factor to consider is the reversibility of protein folding and unfolding. Implementation of a thermodynamic model implies reversible transitions. As indicated in Figures S2 and S3, when heated from room temperature to the T_m value found by DSF and cooled to room temperature, the standard proteins used in this study show no significant change in molar ellipticity by circular dichroism (CD) spectroscopy.

Having demonstrated applicability of the DSF approach to calculating $\Delta_u G°$, $\Delta_u S°$, and $\Delta_u H°$ values we turned toward a study of the pH stability of the cellulase *Fn*Cel5a and a series of its mutants, to highlight the potential of this DSF method as a technique for studying a library of

proteins under a variety of conditions. *Fn*Cel5a is a thermostable cellulase with potential for application in biofuel production[44,45]. DSF thermal stability curves (Figure 3) identify significant decreases in T_m for samples buffered below pH 4 and above pH 9, Taking T_m as a proxy for stability, the data suggests that *Fn*Cel5a is less stable in low or very high pH environments. However, this data does not identify whether these changes in thermal stability are due to entropic or enthalpic effects.

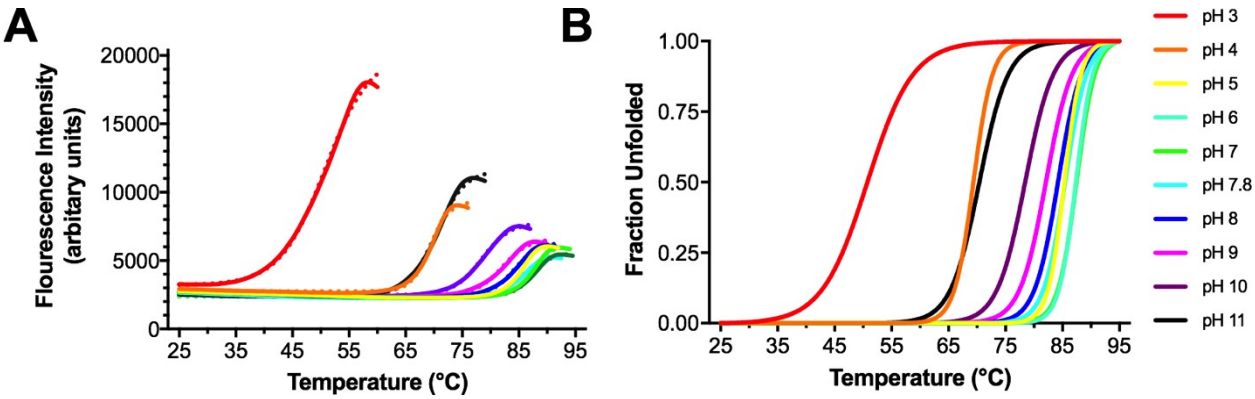

Figure 3. Differential Scanning Fluorimetry of Wild Type Cellulase at various pH values was used to examine the effect of pH on T_m, $\Delta_u G$, $\Delta_u S$, and $\Delta_u H$ of the protein. (A) DSF curves for wild type cellulase *Fn*Cel5a at pH values between 3 and 11. (B) DSF curves allow for calculation of the fraction of protein folded at each temperature.

Utilizing the approach outlined above, we determined $\Delta_u G°$, $\Delta_u S°$, and $\Delta_u H°$ values for wild type *Fn*Cel5a at pH values ranging from 3 to 11 (Table 2, Figure 4). We followed this analysis with a complementary study of the *Fn*Cel5a mutants K94C, K190C, and K300C. Thermal stability curves for wild type, K94C, K190C, and K300C as a function of pH suggest that the point mutations have minimal effect upon stability, in comparison to wild type *Fn*Cel5a. However, the power of the DSF analysis presented here is apparent when comparisons of $\Delta_u G°$, $\Delta_u S°$, and $\Delta_u H°$ values are made for each mutant (Figure 4). These comparisons show that each mutation exhibits small, but measurable difference in $\Delta_u G°$, $\Delta_u S°$, and $\Delta_u H°$ values across the measured pH range. Thus, while measurement of T_m provides thermal stability, analysis of T_m values alone does not provide the full picture, and in fact T_m values can mask potentially

significant changes in stability caused by a combination of offsetting entropic and enthalpic effects.

Table 2. Thermal Stability and Thermodynamic data for Wild Type *Fn*Cel5a Cellulase at various pH values.

pH	T_m (°C)	$\Delta_u G$ (kJ/mol)[a]	$\Delta_u S$ (kJ/mol K)[a]	$\Delta_u H$ (kJ/mol)[a]
3	50.8 ± 0.2	16.0 ± 0.4	0.62 ± 0.02	201 ± 5
4	69.4 ± 0.1	60 ± 2	1.35 ± 0.05	460 ± 20
5	85.4 ± 0.1	86 ± 1	1.42 ± 0.02	511 ± 6
6	87.4 ± 0.1	92 ± 3	1.47 ± 0.05	530 ± 20
7	87.5 ± 0.1	81 ± 1	1.30 ± 0.02	467 ± 6
8	84.2 ± 0.1	63 ± 2	1.06 ± 0.03	380 ± 10
9	82.1 ± 0.1	55 ± 2	0.96 ± 0.04	340 ± 10
10	78.5 ± 0.1	53 ± 1	0.99 ± 0.02	348 ± 7
11	70.5 ± 0.1	43.4 ± 0.9	0.95 ± 0.02	327 ± 7

[a]$\Delta_u G$, $\Delta_u S$, and $\Delta_u H$ are the Gibbs free energy of unfolding, entropy of unfolding, and enthalpy of unfolding, respectively.

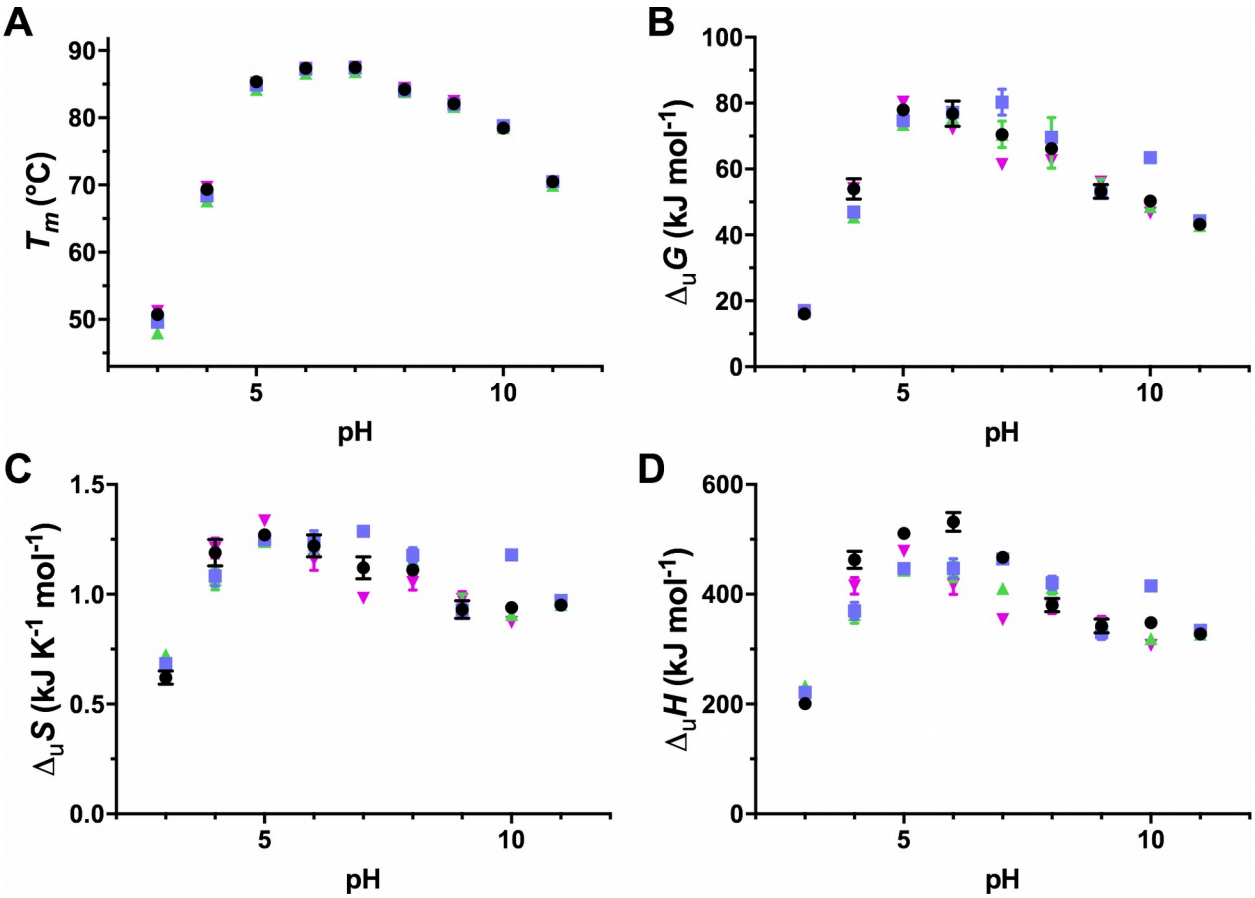

Figure 4. Effect of pH upon the (A) melting temperature, (B) Gibbs free energy of unfolding ($\Delta_u G$), (C) entropy of unfolding ($\Delta_u S$), and (D) enthalpy of refolding ($\Delta_u H$) for *Fn*Cel5a$_{wt}$ (black circles), *Fn*Cel5a$_{K94C}$ (blue squares), *Fn*Cel5a$_{K190C}$ (green triangles), and *Fn*Cel5a$_{K300C}$ (purple triangles).

The present study introduces a facile, simple, and scalable method of calculating Gibbs free energy of unfolding ($\Delta_u G°$), entropy of unfolding ($\Delta_u S°$), and enthalpy of unfolding ($\Delta_u H°$) values. Determining thermodynamic parameters of unfolding via DSF provides significant advantages such as the capacity of an intrinsically parallelized assay in a 96-well format that enables examining multiple conditions simultaneously, and the minimal requirements for protein concentration. The analysis approach presented here transforms DSF from a simple evaluation of T_m values to an experimental method that provides a robust comparison of thermodynamic parameters. This approach gives researchers the capacity to quickly analyze the biophysical

mechanisms that underlie protein stability and to more easily and thoroughly characterize the effect of additives, inhibitors, or pH.

ASSOCIATED CONTENT

Supporting Information. List of materials, *Fn*Cel5a expression and purification protocols, differential scanning fluorimetry data acquisition parameters. (PDF)

AUTHOR INFORMATION

Notes

The authors declare no competing financial interests.

ACKNOWLEDGMENT

The authors acknowledge financial support from the US National Science Foundation (Award No. MCB 1552113 to RCP), the American Heart Association (Award No. 16SDG26960000 to RCP), and institutional support from Miami University (to TAW, JMS, RCP, and DK).

REFERENCES

1. Gummadi, S. N. What is the role of thermodynamics on protein stability. *Biotechnol. Bioprocess Eng.*, **2003**, 8, 9-18.
2. Moosavi-Movahedi, A. A.; Nazari, K. Denaturation of Horseradish Peroxidase with Urea and Guanidine Hydrochloride. *Int. J. Biol. Macromol.* **1995**, *17* (1), 43–47.
3. Venkatesu, P.; Lee, M.-J.; Lin, H.-M. Osmolyte Counteracts Urea-Induced Denaturation of Alpha-Chymotrypsin. *J. Phys. Chem. B* **2009**, *113* (15), 5327–5338.
4. Greene, R. F.; Pace, C. N. Urea and Guanidine Hydrochloride Denaturation of Ribonuclease, Lysozyme, Alpha-Chymotrypsin, and Beta-Lactoglobulin. *J. Biol. Chem.* **1974**, *249* (17), 5388–5393.
5. Kumar, A.; Attri, P.; Venkatesu, P. Trehalose Protects Urea-Induced Unfolding of Alpha-Chymotrypsin. *Int. J. Biol. Macromol.* **2010**, *47* (4), 540–545.
6. Ahmad, F.; Yadav, S.; Taneja, S. Determining Stability of Proteins From Guanidinium Chloride Transition Curves. *Biochem. J.* **1992**, *287* (2), 481–485.
7. Wu, M.-J.; Jiang, Y.; Yan, Y.-B. Impact of the 237th Residue on the Folding of Human Carbonic Anhydrase II. *Int J Mol Sci* **2011**, *12* (5), 2797–2807.
8. Moosavi-Movahedi, A. A.; Nazari, K.; Saboury, A. A. Thermodynamics of Denaturation of Horseradish Peroxidase with Sodium N-Dodecyl Sulphate and N-Dodecyl

Trimethylammonium Bromide. *Colloids Surf B Biointerfaces* **1997**, *9* (3-4), 123–130.
9. Rodríguez Martínez, J. A.; Solá, R. J.; Castillo, B.; Cintrón Colón, H. R.; Rivera Rivera, I.; Barletta, G.; Griebenow, K. Stabilization of A-Chymotrypsin Upon PEGylation Correlates with Reduced Structural Dynamics. *Biotechnol. Bioeng.* **2008**, *101* (6), 1142–1149.
10. Matulis, D.; Kranz, J. K.; Salemme, F. R.; Todd, M. J. Thermodynamic Stability of Carbonic Anhydrase: Measurements of Binding Affinity and Stoichiometry Using ThermoFluor. *Biochemistry* **2005**, *44* (13), 5258–5266.
11. Larsericsdotter, H.; Oscarsson, S.; Buijs, J. Thermodynamic Analysis of Lysozyme Adsorbed to Silica. *J Colloid Interface Sci* **2004**, *276* (2), 261–268.
12. Haque, I.; Singh, R.; Moosavi-Movahedi, A. A.; Ahmad, F. Effect of Polyol Osmolytes on DeltaG_D, The Gibbs Energy of Stabilisation of Proteins at Different pH Values. *Biophys. Chem.* **2005**, *117* (1), 1–12.
13. Ciulli, A. Biophysical Screening for the Diversity of Small-Moleule Ligands. *Methods Mol Biol.* **2013**, 1008, 357-388.
14. Wang, T.; Wade, R. C. On the use of Elevated Temperature in Simulations to Study Protein Unfolding Mechanism. *J. Chem. Theory Comput.* **2007**, 3, 1476-1483.
15. Chiu, M.H.; Prenner, E.J. Differential Scanning Calorimetry: An invaluable took for a detailed thermodynamic characterization of macromolecules and their interactions. *J. Pharm Bioallied. Sci.* **2011**, 3, 39-59
16. Haifeng, L.; Yuwen, L.; Xiaomin, C.; Zhiyong, W.; Cunxin, W. Effects of Sodium Phosphate Buffer on Horseradish peroxidase. *J. Therm. Anal Calorim.* **2008**, 93, 569-574
17. Cho, T. Y.; Byrne, N.; Moore, D. J.; Pethica, B. A.; Angell, C. A.; Debenedetti, P. G. Structure-energy relations in hen egg white lysozyme observed during refolding from a quenched unfolded state. *Chem. Commun.* **2009**, 4441-4443
18. Amani, M.; Khodarahmi, R.; Ghobadi, S.; Mehrabi, M.; Kurganov, B. I.; Moosavi-Movahedi, A. A. Differential Scanning Calorimetry Study on Thermal Denaturation of Human Carbonic Anhydrase II. *J. Chem. Eng. Data* **2011**, 56, 1158-1162
19. Segar, S.L.; Beitle, R. R.; Ataai, M. M.; Domach, M.M. Metal-based affinity separation of alpha- and gamma- chymotrypsin and thermal stability analysis of isolates. *Bioseparation* **1992**, 3, 5, 291-296
20. Ericsson, U.B., Hallberg, B.M., DeTitta, G.T., Niek Dekker, N., and Nordlund, P. Thermofluor-based high-throughput stability optimization of proteins for structural studies. *Anal. Biochem.* **2006**, 357, 2, 289-298.
21. Lucius, M.; Falatach, R.; McGlone, C.; Makaroff, K.; Danielson, A.; Williams, C.; Nix, J. C.; Konkolewicz, D.; Page, R.C.; Berberich, J.A. Investigating the impact of polymer functional groups on the stability and activity of lysozyme-polymer conjugates. *Biomac.* **2016**, 17, 1123-1134
22. Niesen, F.H.; Berglund, H.; Vedadi, M. The use of differential scanning fluorimetry to detect ligand interactions that promote protein stability. *Nature Protocols.* **2007**, 2, 2212-2221
23. Bommarius, A. S.; Paye, M. F. Stabilizing biocatalysts. *Chem. Soc. Rev.* **2013**, 42, 6534 – 6565
24. Safarian, S.; Saffarzadeh, M.; Zargar, S. J.; Moosavi-Movahedi, A. A. Molten Globule-Like State of Bovine Carbonic Anhydrase in the Presence of Acetonitrile. *J. Biochem.* **2006**, 139(6), 1025-1033
25. Greenfield, N. J. Using circular dichroism collected as a function of temperature to determine the thermodynamics of protein unfolding and binding interactions. *Nat Protoc.* **2006**, 1, 2527-2535
26. Venkataramani, S.; Truntzer, J.; Coleman, D. R. Thermal stability of high concentration lysozyme across varying pH: A Fourier Transform Infrared study. *J. Pharm Bioallied Sci.* **2013**, 5(2), 148 -153

27. Knubovets, T.; Osterhout, J.J.; Klibanov, A. M. Structure, thermostability, and conformational flexibility of hen egg-white lysozyme dissolved in glycerol. *PNAS* **1999**, 96(4), 1262-1267
28. Farhadian, S.; Shareghi, B.; Saboury, A.A.; Babheydari, A. K.; Raisi, F.; Heidari, E. Molecular aspects of the interaction of spermidine and α-chymotrypsin. *Int. J. Biol. Macromolecules* **2016**, 92, 523-532.
29. Wu, M.; Jiang, Y.; Yan, Y. Impact of the 237th Residue of the folding of Human Carbonic Anhydrase II. *Int. J. Mol. Sci.* **2011**, 12, 2797-2807
30. Teles, R. C. L.; Calderon, L. A., Medrano, F. J.; Barbosa, J. A. R. G.; Guimarães, B. G.; Santoro, M. M.; Freitas, S. M. pH dependence Thermal Stability of a Chymotrypsin Inhibitor from Schizolobium parahyba seeds. *Phytochem.* **2004**, 65(7), 793-799
31. Yue, Q.; Niu, L.; Li, X.; Shao, X.; Xie, X.; Song, Z. Study of the Interaction Mechanism of Lysozyme and Bromophenol Blue by Fluorescence Spectroscopy. *J. Fluoresc.* **2008**, 18, 11-15
32. Diego, T. D.; Lozano, P.; Gmouh, S.; Vaultier, M. Iborra, J. L. Fluorescence and CD spectroscopic analysis of the ALPHA-chymotrypsin stabilization by the ionic liquid, 1-ethyl-3-methylimidazolium bis[(trifluoromethyl)sulfony]amide. *Biotechnol Bioeng.* **2004**, 88, 916-924
33. Pace, C. N.; Scholtz, J. M. Measuring the Conformational Stability of a Protein. *Protein structure: A practical approach* **1997**.
34. Bye, J. W.; Falconer, R. J. Thermal Stability of lysozyme as a function of ion concentration: A reappraisal of the relationship between the Hofmeister series and protein stability. *Protein Science.* **2013**, 22, 1563-1570.
35. Bushmarina, N.A.; Kuznetsova, I. M.; Biktashev, A. G.; Turoverov, K. K.; Uversky, V. N. Partially folded conformations in the folding pathway of bovine carbonic anhydrase II: a fluorescence spectroscopic analysis. *Chembiochem.* **2001**, 2(11), 813-821
36. McCoy, Jr. L. F.; Rowe, E. S.; Wong, K. Multiparameter kinetic study on the unfolding and refolding of bovine carbonic anhydrase B. *Biochemistry* **1980**, 19, 4738-4743
37. Kiefhaber, T. Kinetic traps in lysozyme folding. *PNAS* **1995**, 92 (20), 9029-9033
38. Gladwin, S. T.; Evans, P. A. Structure of very early protein folding intermediates: new insights through a variant of hydrogen exchange labelling. *Folding & Design* **1996**, 1, 407-417
39. Biggar, K.K.; Dawson, N. J.; Storey, K. B. Real-time protein unfolding: a method for determing the kinetics of native protein denaturation using a quantitative real-time thermocycler. *BioTechniques* **2012**, 53, 231-238
40. Hawe, A.; Sutter, M.; Jiskoot, W. Extrinsic Fluorescent Dyes as Tools for Protein Characterization. *Pharm. Res.* **2008**, *25* (7), 1487–1499.
41. Prabhu, N. V.; Sharp, K. A. Heat Capacity in Proteins. *Annu. Rev. Phys. Chem.* **2005**, 56, 521-48
42. Gitlin, I.; Gudiksen, K. L.; Whitesides, G. M. Effects of Surface Charge on Denaturation of Bovine Carbonic Anhydrase. *Chembiochem* **2006**, *7* (8), 1241–1250.
43. Attri, P.; Venkatesu, P. Exploring the Thermal Stability of A-Chymotrypsin in Protic Ionic Liquids. *Process Biochemistry* **2013**, *48* (3), 462–470.
44. Galbe, M.; Zacchi, G. Pretreatment of Lignocellulosic Materials for Efficient Bioethanol Production. *Biofuels* **2007**, 108, 41-65
45. Hallac, B.B.; Sannigrahi, P.; Pu, Y.; Ray, M.; Murphy, R. J.; Ragauskas, A. J. Biomass Characterization of Buddleja davidii: A potential feedstock for Biofuel production. *J. Agric. Food Chem.* **2009**, 57, 1275-1281